General Disclaimer

One or more of the Following Statements may affect this Document

- This document has been reproduced from the best copy furnished by the organizational source. It is being released in the interest of making available as much information as possible.

- This document may contain data, which exceeds the sheet parameters. It was furnished in this condition by the organizational source and is the best copy available.

- This document may contain tone-on-tone or color graphs, charts and/or pictures, which have been reproduced in black and white.

- This document is paginated as submitted by the original source.

- Portions of this document are not fully legible due to the historical nature of some of the material. However, it is the best reproduction available from the original submission.

AMPEX

GPO PRICE $ _____

CFSTI PRICE(S) $ _____

Hard copy (HC) 3.00

INDEX

0475
1725
2545
2589
2732
6104
6194

UNCLASSIFIED

Distribution

Prepared under

Contract NASW-1456
National Aeronautics and
Space Administration
Washington, D.C.

STUDY, FABRICATION, AND TESTING OF A FOIL BEARING ROTOR SUPPORT SYSTEM

Quarterly Report
Period Ending November 15, 1966

RR 66-38

Approved by _____
M. Wildmann, Section Manager
Manager, Mechanics Section

Approved by _____
W. A. Gross,
Director of Research

AMPEX CORPORATION

RESEARCH AND ENGINEERING PUBLICATION

CONTENTS

NOMENCLATURE

a	Distance between shaft center and the line of support under no rotation, no load conditions
b	Half-width of line of supports
E	Modulus of elasticity of foil
h^*	Nominal clearance under foil
h_e	Distance of asymptote to shaft at exit
h_i	Distance of asymptote to shaft at inlet
ℓ_o	Unstrained total foil length
ℓ_e	Length of exit branch of tape
ℓ_i	Length of inlet branch of tape
m	Mass of shaft
O	Origin of shaft center under no load, no rotation conditions
r_o	Radius of shaft
t_o	Characteristic time
t	Foil thickness
T	Foil tension per unit width
W	Load on shaft (considered perpendicular to line of supports)
x	Displacement from origin parallel to line of supports (positive if in direction of inlet)
y	Displacement from origin perpendicular to line of supports (positive when away from foil)

α	Angle between the exit branch of the foil and line of supports
β	Angle between the inlet branch of the foil and line of supports
ΔT	Total fluid shear per unit width on foil
τ	Dimensionless time = (time/t_o)

1.0 INTRODUCTION

In the previous phase of the program, the feasibility of supporting a high-speed rotor on foil bearings was demonstrated. It appears that this type of support is free from the destructive "half-frequency whirl" instability.

During the reporting quarter, work on the following has begun and is in progress at the the present time:

(1) Runs of moderate duration are being conducted on the existing test rig.

(2) Design of apparatus to:

  (a) test methods of starting
  (b) investigate the response of the foil rotor system to external excitation.

(3) An orbit program directed toward improving our understanding of the system and for the prediction of its behavior is being developed.

2.0 EXPERIMENTS ON EXISTING RIG

The existing foil supported rotor test apparatus was used to investigate foil wear problems that have occurred in our past work. Previously, it had been noted that contact had occurred in the entrance region as well as what appeared to be metal fatigue in the exit region.

For the test run, the foil tension was 2.0 lb/in., and the total wrap angle was 150°. After liberally wetting the rotor surface with Freon, the rotor was started. The running speed of 60,000 rpm was maintained for more than an hour. The test rig was then disassembled.

The lower foils showed no sign of contact or fatigue. The upper foils showed very light and even contact in the constant gap region, a light debris buildup in the exit region, and they, too, showed no sign of fatigue. The rotor showed very light contact on both planes of the bearing.

Since there were no visible signs of contact in the entrance region after one four of running and one start-stop cycle, it is assumed that the contact and fatigue noted in earlier experiments were caused by the repeated start-stop cycles to which the foils had been subjected during these earlier runs. That the upper foils showed contact while the lower did not was probably the result of the shaft being located axially by the use of a single thrust bearing at the bottom.

3.0 DESIGN OF NEW APPARATUS

3.1 Methods of Starting

There are essentially three methods of attack:

(1) Starting with tension of foil relaxed;

(2) Starting under tension and minimizing the starting torque by coating or plating the foils with materials having low friction coefficients and good wear compatibility with the rotor;

(3) Starting with foils under external pressurization while the rotor is brought up to speed.

The first method has several disadvantages. The rotor would have to be supported during the accelerating period on solid stable bearings. The latter would have to be retracted and tension would have to be applied simultaneously to the foils once the rotor had reached operating speed. The complexity of mechanism required to achieve this condition is incompatible with the simplicity aimed for in using a foil rotor system.

The second method, though imperfect, will be investigated. Promising platings and/or coatings will be tried. We shall measure the starting torques and investigate surface wear compatibility under start-stop conditions.

The third method involves using an external pressure source during the period of rotor acceleration, in a time interval sufficiently long for the rotor to gain enough speed to establish self-acting support. Though more elaborate than "dry starting," the method is both feasible and practical. Nor are the mass of gas and the size of gas storage container prohibitive to ensure a limited number of friction-free starts.

A compact apparatus is being designed to investigate the third method of starting. In order to limit the motion to one plane and the radial support to a single set of three foils, a stubby shaft will be mounted between two externally pressurized thrust bearings. These bearings will be sufficiently stiff to minimize pitching and to exclude resonances from the operating speed range. The separation of the stationary rotor from the foils is to be achieved by supplying air through two rows of orifices from the interior of the rotor. Noncontact seals at the rotor thrust faces will prevent excessive leakage during pressurization, as well as from the air film under operating conditions. The air supply is cut off when the rotational speed is high enough to generate sufficient self-support of the rotor.

Motion will be imparted by two impulse wheels, integral with the rotor and straddling the foils. The design will allow for one or more methods of mounting and of applying tension to the foils. A schematic diagram of the apparatus now being designed is shown in Fig. 1. A simple, auxiliary test rig is being constructed to test the effectiveness of lifting the foil by external pressurization and to test a specific method of foil attachment and tensioning.

3.2 Dynamic Response of Foil Rotor System

The experimental apparatus, shown schematically in Fig. 1, will be compact, with provision made for attaching it to a shake table. The response of the foil rotor system to excitations in directions normal to the rotor axis will be monitored at various frequencies of excitation and at representative rotational speed and tension levels.

Once the starting problem is satisfactorily solved and sufficient information is gathered with regard to the dynamics of a rotor mounted on a single set of foils, a basis will be provided for the construction of a prototype system referred to at Phase II of the proposal.

4.0 ORBIT PROGRAM

The best approach appears to be constructing the orbit program step by step with increasing complexity:

4.1 Single-Foil Model

The simplest model is a shaft supported on a single foil as in Fig. 2. The film is considered quasi-static and offers no damping. The restoring forces consist of a series of nonlinear springs. The basic equations are given in the Appendix.

An orbit program based on these equations has been debugged, and a preliminary result of the orbit following displacement of the shaft from its equilibrium position is given in Fig. 3.

4.2 Three-Foil Rotor Support

The above idea of the single-foil rotor support has been generalized to the case of three foils, and a corresponding orbit program is presently in the process of debugging.

APPENDIX

EQUATIONS FOR THE SINGLE-FOIL ROTOR SUPPORT

The momentum equations for the shaft are

$$\left(\frac{T}{Et} + \frac{\Delta T}{Et}\right)\cos\beta - \frac{T}{Et}\cos\alpha = \frac{m r_o}{Et\, t_o^2}\frac{d^2(x/r_o)}{d\tau^2} \tag{1}$$

$$-\frac{W}{Et} + \left(\frac{T}{Et} + \frac{\Delta T}{Et}\right)\sin\beta + \frac{T}{Et}\sin\alpha = \frac{m r_o}{Et\, t_o^2}\frac{d^2(y/r_o)}{d\tau^2} \tag{2}$$

The stress-strain relation is

$$\frac{T}{Et} = \frac{\left[\frac{\ell_i}{r_o} + \left(1 + \frac{h^*}{r_o}\right)(\alpha+\beta) + \frac{\ell_o}{r_o}\right] - \frac{\ell_o}{r_o}}{\frac{\ell_o}{r_o}} \tag{3}$$

From geometry,

$$\frac{\ell_i}{r_o} = \sqrt{\left(\frac{a}{r_o} - \frac{y}{r_o}\right)^2 + \left(\frac{b}{2r_o} + \frac{x}{r_o}\right)^2 - \left(1 + \frac{h^*}{r_o}\right)^2} \tag{4}$$

$$\frac{f_2}{r_o} = \sqrt{\left(\frac{a}{r_o} - \frac{y}{r_o}\right)^2 + \left(\frac{b}{2r_o} - \frac{x}{r_o}\right)^2 - \left(1 + \frac{h^*}{r_o}\right)^2} \tag{5}$$

$$\alpha = \operatorname{arctg}\left(\frac{\frac{a}{r_o} - \frac{y}{r_o}}{\frac{b}{2r_o} + \frac{x}{r_o}}\right) + \arcsin\left(\frac{1 + \frac{h_e}{r_o}}{\sqrt{\left(\frac{x}{r_o} + \frac{b}{2r_o}\right)^2 + \left(\frac{a}{r_o} - \frac{y}{r_o}\right)^2}}\right) \tag{6}$$

$$\beta = \operatorname{arctg}\left(\frac{\frac{a}{r_o} - \frac{y}{r_o}}{\frac{b}{2r_o} - \frac{x}{r_o}}\right) + \arcsin\left(\frac{1 + \frac{h_i}{r_o}}{\sqrt{\left(\frac{b}{2r_o} - \frac{x}{r_o}\right)^2 + \left(\frac{a}{r_o} - \frac{y}{r_o}\right)^2}}\right) \tag{7}$$

The film stiffness is determined from:

$$\frac{h^*}{r_o} = 0.643 \left(\frac{6\mu U}{Et}\right)^{2/3} \Big/ \left(\frac{T}{Et}\right)^{2/3} \tag{8}$$

$$\frac{h_i}{r_o} = 1.811 \left(\frac{6\mu U}{Et}\right)^{2/3} \Big/ \left(\frac{T}{Et}\right)^{2/3} \tag{9}$$

$$\frac{h_e}{r_o} = -0.416 \left(\frac{6\mu U}{Et}\right)^{2/3} \Big/ \left(\frac{T}{Et}\right)^{2/3} \tag{10}$$

$$\frac{\Delta T}{Et} = \frac{1}{6 \times 0.643} \left(\frac{T}{Et}\right)^{2/3} \left(\frac{6\mu U}{Et}\right)^{1/3} \Theta \tag{11}$$

In the above equations the quantities

$$\frac{W}{Et} \;,\; \frac{mr_o}{Et\cdot t_o^2} \;,\; \frac{6\mu v}{Et} \;,\; \frac{b}{r_o} \;,\; \theta$$

are prescribed dimensionless parameters describing the load, inertia, film, and geometry respectively. The unstrained total foil length ℓ_o and the parameter a may be found from the geometrical relations:

$$\frac{\ell_o}{r_o} = \frac{b}{r_o \cos\frac{\theta}{2}} - 2\,tg\,\frac{\theta}{2} + \theta \qquad (12)$$

$$\frac{a}{r_o} = \frac{b}{2r_o}\,tg\,\frac{\theta}{2} - \frac{1}{\cos\frac{\theta}{2}} \qquad (13)$$

For a given x/r_o, y/r_o, the transcendental equations (Eqs. 3 through 11) are soluble by trial and error and yield values for T/Et, $\Delta t/Et$, α, β. When these values are substituted in the differential equations (Eqs. 1 and 2), the values of the acceleration components are found and the future behavior of the shaft is predicted.

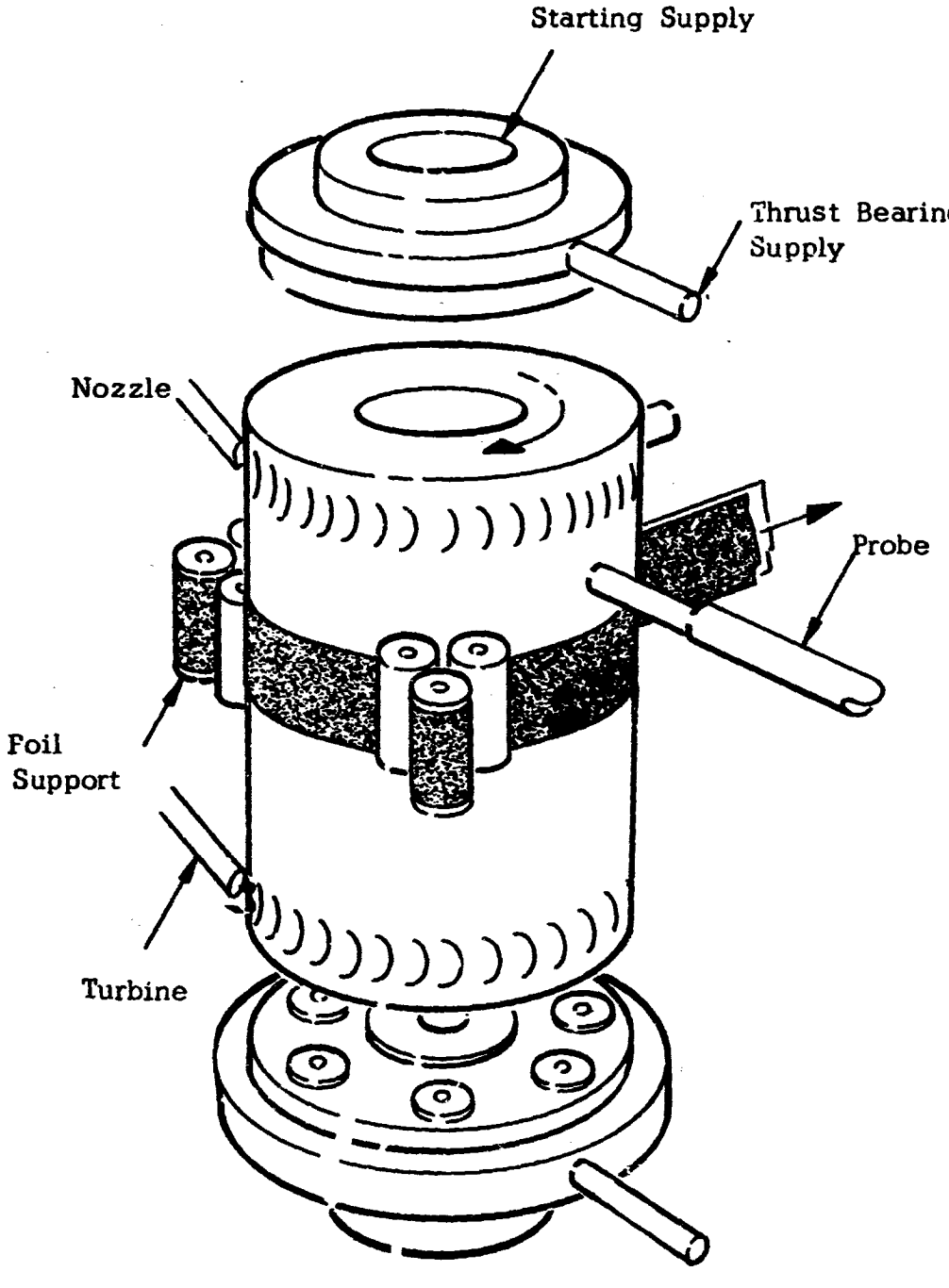

Fig. 1 Schematic Diagram of Apparatus

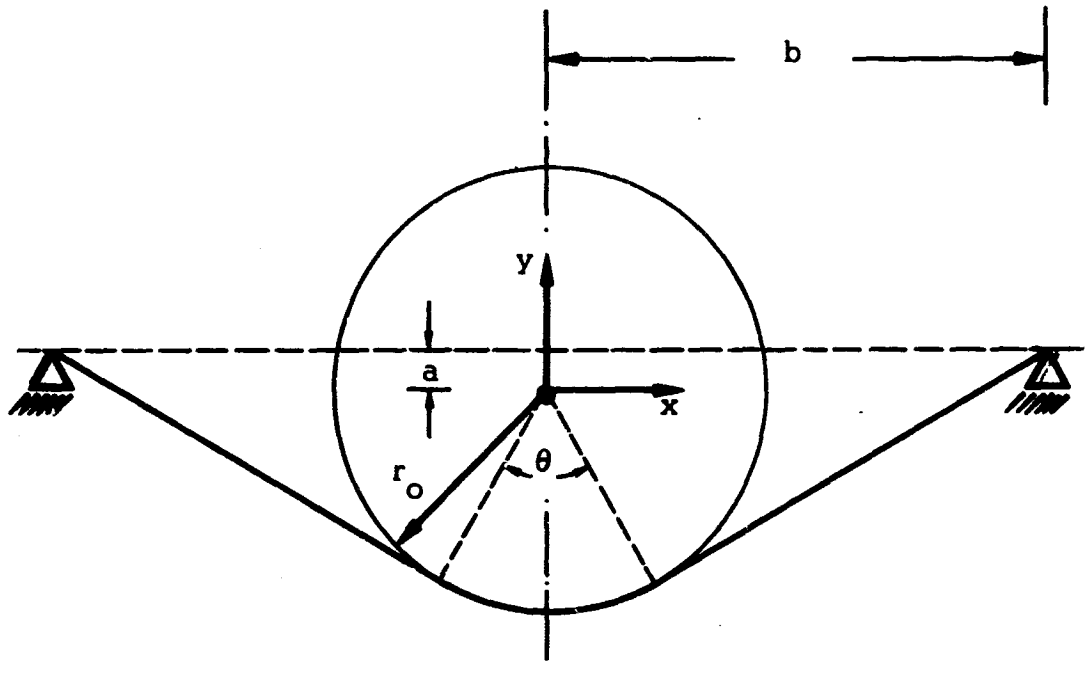

Fig. 2a Shaft at Origin - No Load, No Rotation Condition

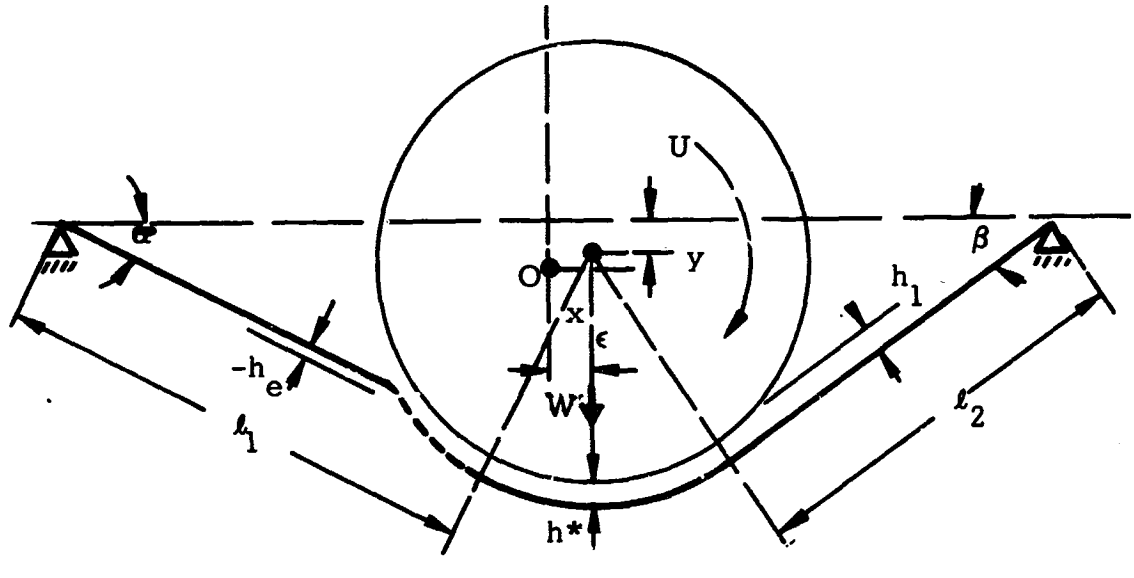

Fig. 2b Shaft Displaced to (x,y)

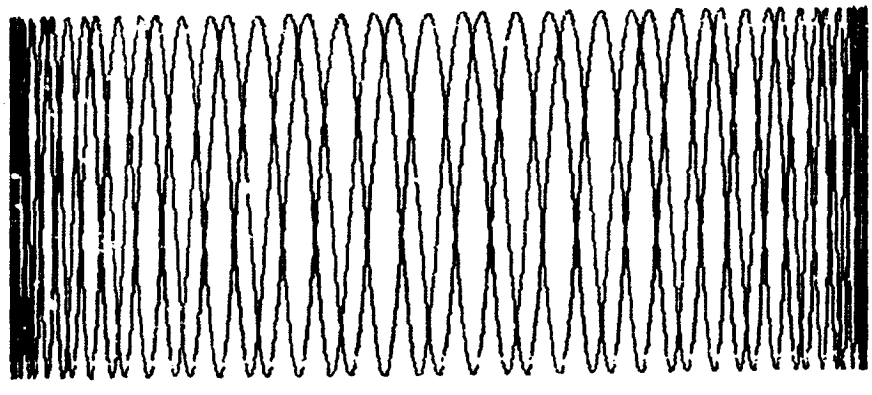

Fig. 3 Orbit of Rotor Supported By Single-Foil. Register Mark at Left Indicates Equilibrium Position in No-Load, No-Rotation Condition